Structural Elements and Limited Proteolysis of CD39 Influence ATP Diphosphohydrolase Activity†

Jan Schulte am Esch II,‡ Jean Sévigny,‡ Elzbieta Kaczmarek,‡ Jonathan B. Siegel,§ Masato Imai,§ Katarzyna Koziak,‡ Adrien R. Beaudoin,|| and Simon C. Robson*,‡,§

Departments of Medicine and Surgery, Beth Israel Deaconess Medical Center, Harvard Medical School, 99 Brookline Avenue, Boston, Massachusetts 02215, and Département de Biologie, Faculté des Sciences, Université de Sherbrooke, Sherbrooke, Québec, Canada J1K 2R1

Received October 12, 1998; Revised Manuscript Received December 10, 1998

ABSTRACT: CD39, the mammalian ATP diphosphohydrolase (ATPDase), is thought to contain two transmembrane domains and five "apyrase conserved regions" (ACR) within a large extracellular region. To study the structure of this ectoenzyme, human CD39 was modified by directed mutations within these ACRs or by sequential deletions at both termini. ATPDase activity was well preserved with FLAG tagging, followed by the removal of either of the demonstrated C- or N-transmembrane regions. However, deletions within ACR-1 (aa 54−61) or -4 (aa 212−220), as well as truncation mutants that included ACR-1, -4, or -5 (aa 447−454), resulted in substantive loss of biochemical activity. Intact ACR-1, -4, and -5 within CD39 are therefore required for maintenance of biochemical activity. Native and mutant forms of CD39 lacking TMR were observed to undergo multimerization, associated with the formation of intermolecular disulfide bonds. Limited tryptic cleavage of intact CD39 resulted in two noncovalently membrane-associated fragments (56 and 27 kDa) that substantially augmented ATPDase activity. Glycosylation variation accounted for minor heterogeneity in native and mutant forms of CD39 but did not influence ATPDase function. Enzymatic activity of ATPDase may be influenced by certain posttranslational modifications that are relevant to vascular inflammation.

The vascular ATP diphosphohydrolase (ATPDase)[1] or CD39 is an integral membrane protein that belongs to the GDA 1/CD39 NTPase family (*1*−*5*). These enzymes require Ca^{2+}/Mg^{2+} and cause the hydrolysis of nucleotide di- and triphosphates (*6*, *7*). This group of proteins comprises certain mammalian (*8*−*11*), invertebrate (*12*), protozoan (*13*), and plant E-type ATPases (*2*) that share sequence homology, with particular reference to "apyrase conserved regions" (ACR) (*2*, *14*).

Although some of these enzymes are inherently soluble (*7*, *15*), the mammalian vascular ATPDase is associated with endothelial cell (EC) membranes (*1*, *4*). Here, the enzyme hydrolyzes extracellular ATP and ADP, which are released following activation of EC and platelets into the blood, to the monophosphate form (*16*, *17*). The latter are then transformed to adenosine through the action of 5′-nucleotidase and exert further modulatory effects upon vascular inflammation and hemostasis (*18*).

Modeling studies and structural analysis of CD39 suggest two transmembrane domains at both the N- and C-termini with a large extracellular loop containing a more central hydrophobic region (*5*). Further, there are six potential N-linked glycosylation sites and a total of 11 cysteine residues that may be implicated in the formation of oligomers (*1*, *5*, *19*). There are also several sites that may be modified by ectoprotein kinases (*6*, *20*) as well as potential intracellular protein kinase C phosphorylation (*6*) and potential palmitoylation sites (K. Koziak, unpublished observations). Other posttranslational changes with oxidation or specific proteolytic cleavages may be of importance in modulating enzymatic function (*21*, *22*).

The nature and composition of the ectonucleotidase catalytic site remains undetermined. The fourth ACR (aa 212−220; ACR-4) is found in both ecto-ATPase and CD39/ATPDase and has high-level homology with actin−HSP 70 β-hexokinase and γ-phosphate binding motifs (*2*, *13*); less sequence similarity has been noted for ACR-1 (aa 54−61). The porcine pancreatic ATPDase appears truncated and therefore to lack ACR-1 to -3 (*1*, *9*). Another potential ACR (termed ACR-5; aa 447−454) in the C-terminal region has been identified by Vasconcelos et al (*12*, *14*).

It is also possible that areas other than the reported ACR may constitute functional catalytic site(s) or influence the differentiation of either ATPase and/or ADPase hydrolytic specificity. The objective of this work was to determine

† This is manuscript 760 from our laboratory. This work was funded by NIH Grant RO1HL57307 and American Heart Association Grant GIA 9650490N. J.S.E. was funded by a postdoctoral fellowship from the Deutsche Forschungsgemeinschaft, and J. Sévigny is a recipient of studentships from the Heart and Stroke Foundation of Canada and Fonds pour la Formation de Chercheurs et l'Aide à la Recherche du Québec. Preliminary data was presented at the 70th American Heart Association Scientific Session in Orlando, FL, 1997.

* Address for correspondence: Room 370H, Research North, Beth Israel Deaconess Medical Center, 99 Brookline Ave., Boston, MA 02215. Tel: (617) 632-0881. Fax: (617) 632-0880. E-mail: srobson@bidmc.harvard.edu.

‡ Department of Medicine, Harvard Medical School.

§ Department of Surgery, Harvard Medical School.

|| Université de Sherbrooke.

[1] Abbreviations: ACR, apyrase conserved regions; ATPDase, ATP diphosphohydrolase; DTT, dithiothreitol; EC, endothelial cell; mAb, monoclonal antibody; TMD, transmembrane domain.

10.1021/bi982426k CCC: $18.00
Published on Web 02/02/1999

relationships between defined structural alterations or post-translational modifications of CD39 and the levels of membrane ATPDase enzymatic activity.

EXPERIMENTAL PROCEDURES

Antibodies. Anti-human CD39 (BU61) monoclonal antibodies (mAb) were purchased from AnCell (Bayport, MN). Anti-mouse and anti-rabbit IgG−FITC conjugates as well as monoclonal mouse M2 anti-FLAG were purchased from Sigma (St. Louis, MO); peroxidase-conjugated anti-rabbit antibodies were purchased and used as recommended (Pierce, Rockford, IL). A 16 amino acid peptide from the N-terminus of the porcine pancreatic ATPDase (KSDTQETYGALDLGGA) with common sequence homology to human CD39 (aa 202−217) was used for the generation of rabbit polyclonal antibody. This polyclonal antibody preparation (RO202/217) has been found to react with human CD39/ATPDase expressed by COS-7 transfectants (*1*). To generate additional antibodies (KY102/130), a high-density multigenic peptide system (MAPS) was synthesized with peptides corresponding to amino acid sequence 102−130 of human CD39 (*5*). This approach used a small peptidyl core matrix of four lysine residues bearing four branching peptides (Service de séquence de peptide de l'Est du Québec). Rabbits were immunized and antibodies characterized as previously described (*10, 11*).

Cell Culture. Human umbilical vein endothelial cells (HUVEC) from fresh umbilical veins were cultured in M199 with 20% FCS, heparin (100 μg/mL), and endothelial cell growth factor (50 μg/mL) (BioWhittaker, Walkersville, MD); COS-7 cells were cultured in Dulbecco's modified Eagle's medium (DMEM) with 10% FCS. Both media were supplemented with L-glutamine (2 mM), penicillin G (100 units/mL), and streptomycin (100 μg/mL) (*1*). All cells were grown in culture dishes at 37 °C in a humidified incubator with a 5% CO_2 atmosphere. Cultured cells were harvested by scraping; EC were used at passage 3.

Preparation of CD39/ATPDase ACR-1 or ACR-4 Deletion Mutants by Overlap Extension Using the Polymerase Chain Reaction (PCR). RNA isolated from human umbilical vein endothelial cells served as a template for reverse transcriptase−PCR (*1*). To prepare CD39 ACR-1 and ACR-4 deletion mutants, we employed site-directed mutagenesis by overlap extension using PCR (*23*). Two separate amplifications were required with two complementary oligodeoxyribonucleotide mutant primers. In the first PCR reaction, 5′-flanking primer (5′-ATA ATA GGA TCC ATG GAA GAT ACA AAG GAG-3′) and antisense mutant primers (5′-ATA GAT GTA TAA ACT TGT GTG AAT CCC ATA CTT AAC GTT-3′ and 5′-TTG GGG TAC AAA AGT GAC TTG AAA GGT TTC CTG ATT ATT-3′) for ACR-1 and -4, with annealing temperatures of 48 and 54 °C, respectively, were used. In the second amplification reaction, the sense mutant primers (5′-CAC ACA AGT TTA TAC ATC TAT-3′ and 5′-CAA GTC ACT TTT GTA CCC CAA-3′), for ACR-1 and ACR-4, with annealing temperatures of 48 and 54 °C, respectively, and the 3′-flanking primer (5′-ATA ATA TCT AGA TCA CTT GTC GTC ATC GTC TTT GTA GTC TAC CAT ATC TTT CCA GAA ATA TG-3′) were applied. The latter was designed to introduce the coding sequence for a C-terminal FLAG tag of the protein for later immunological detection. As the result of these amplifications two overlapping mutant fragments were generated, one with a mutation at the 3′ end and another with the same mutation at its 5′ end. Generated fragments were gel purified with a Qiaex II DNA extraction kit (Qiagen, Santa Clarita), and both were used as a template in another PCR reaction with 5′- and 3′-flanking primers (as above). The reactions were carried out in MJ Research Thermal Cycler (Watertown, MA) for 35 cycles (0.5 min at 94 °C; 1 min at 57 °C; 2 min at 72 °C) followed by 10 min at 72 °C. Amplified PCR products were examined on 1% agarose gel and then sequenced (automated sequenator, Applied Biosystems (ABI), Foster City, CA) to confirm the absence of nucleotides 221−241 (ACR-1) and 695−724 (ACR-4), respectively.

CD39 Expression Vectors. For expression of native CD39, an identical approach as described previously was used (*1*). For N-terminal and double-truncated forms of CD39, a vector based on the pcDNA3 plasmid was designed to ensure membrane expression of the protein with attachment of the unique eight amino acids spanning FLAG tag (DYKDDDDK). For this purpose the mouse pre-protrypsin leader as a secretory sequence including the translational initiation signal, a *Hin*dIII restriction site at the 5′ end, and a *Bam*HI site at the 3′ end were ligated at the 5′ end of the construct as described previously (*24*). In addition, the sequence included the DNA sequence coding for the FLAG epitope. The sequences for these synthetic oligonucleotides were previously published (*24*). Each truncated mutation was generated by PCR using either cDNA as described above or 0.25 μg of a CD39-pcDNA3 vector, described previously (*1*) with an annealing temperature of 55−57 °C and 25−30 cycles. All the oligonucleotides used for generation of the truncated forms of CD39, as well as FLAG-tagged CD39, are shown in Table 1. PCR products were gel-cleaned, digested, and ligated into the polylinker of the vector utilizing a *Bam*HI site at the 5′ end and a *Xba*I site at the 3′ end for FLAG-tagged CD39 as well as N- and C-terminal truncations and a *Eco*RI site at the 3′ end for double truncations, respectively. The pcDNA3 vectors were utilized for C-terminal truncations and the FLAG-tagged native protein. To ensure attachment of a FLAG tag in C-terminal truncated forms and FLAG-tagged CD39, the antisense primer used for PCR included the nucleotide sequence coding for FLAG. To achieve GPI-anchored membranous expression of the double-truncated forms of CD39, synthetic oligonucleotides were ligated at the 3′ end of the protein-coding sequence containing nucleotides coding for the last 37 amino acids of decay accelerating factor (DAF). This measure provided a signal for covalent attachment of a GPI membrane anchor; the sequences of these synthetic oligonucleotides containing a stop codon, an *Eco*RI restriction site (5′ end), and a *Not*I restriction site (3′ end) were exactly as published (*24*). Constructs in expression vectors were sequenced using an ABI 373 fluorescent DNA sequencer (ABI) using SP6 and T7 primers as well as custom sequencing primers.

Transient Transfection. DNA (85 ng of vector/cm^2 culture plate surface area) was precipitated with 0.3 M sodium acetate, pH 7.0, and 70% ethanol at −80 °C for 1 h before incubation with lipofectamine (3 μg/cm^2) for 30 min at room temperature. COS-7 cells, at 80% confluence, were incubated with the DNA/lipofectamine mixture for 5 h at 37 °C in serum-free medium. The transfection was then terminated

Table 1: Sequences of Primer Used for PCR Amplification of Truncated Mutants[a]

Mutant	Oligonucleotides for PCR (upper lane - sense primer / lower lane - antisense primer)
WILD TYPE tagged	5'ata ata gga tcc atg gaa gat aca aag gag 5'ata ata tct aga tca ctt gtc gtc atc gtc ttt gta gtc tac cat atc ttt cca gaa ata tg
NT-Δ-1-37	5'tat taa gga tcc gac cca gaa caa agc att gc 5'tat taa tct aga ttg cta tac cat atc ttt cc
NT-Δ-1-61	5'tat taa gga tcc ttt ata cat cta taa gtg gc 5'tat taa tct aga ttg cta tac cat atc ttt cc
NT-Δ-1-202	5'tat taa gga tcc aac caa taa tca gga aac ct 5'tat taa tct aga ttg cta tac cat atc ttt cc
NT-Δ-1-220	5'tat taa gga tcc agt cac ttt tgt acc cc 5'tat taa tct aga ttg cta tac cat atc ttt cc
CT-Δ-477-510	5'ata ata gga tcc atg gaa gat aca aag gag 5'ata ata tct aga tca ctt gtc gtc atc gtc ttt gta gtc ggt gga gtg gga gag agg tgt gg
CT-Δ-329-510	5'ata ata gga tcc atg gaa gat aca aag gag 5'ata tta tct aga tta ctt gtc gtc atc gtc ttt gta gtc ttg tgt aga ggc tcc ccc aag g
CT-Δ-305-510	5'ata ata gga tcc atg gaa gat aca aag gag 5'ata tta tct aga tta ctt gtc gtc atc gtc ttt gta gtc ctt ccc ata gca caa gaa gc
CT-Δ-286-510	5'ata ata gga tcc atg gaa gat aca aag gag 5'ata tta tct aga tta ctt gtc gtc atc gtc ttt gta gtc agg atg aaa gca tgg gtc cc
CT-Δ-259-510	5'ata ata gga tcc atg gaa gat aca aag gag 5'ata tta tct aga tta ctt gtc gtc atc gtc ttt gta gtc tct ctt ggt gca ggg ggt ctt g
CT-Δ-221-510	5'ata ata gga tcc atg gaa gat aca aag gag 5'ata tta tct aga tta ctt gtc gtc atc gtc ttt gta gtc gct ttg atg gca ttg ttg ata g
DT-Δ-1-37/Δ-477-510	5'tat taa gga tcc gac cca gaa caa agc att gc 5'att ata gaa ttc ggt gga gtg gga gag agg tg
DT-Δ-1-37/Δ-221-510	5'tat taa gga tcc gac cca gaa caa agc att gc 5'tat taa gaa ttc ttg tgt aga ggc tcc ccc aag

[a] The nomenclature of the mutants is as defined in Figure 1.

by addition of FCS to a final concentration of 10%. The medium was changed after 48 h, and cells were harvested for assays or purification after 72 h. Both control COS-7 cells used for transfection and empty vector transfected cells were negative for CD39 as analyzed by Western blotting and FACS with anti-CD39; in both controls ATPDase activity was negligible.

Cytofluorometric Analysis. Transfected cells suspended in phosphate-buffered saline (Dulbecco's PBS−Mg^{2+}−Ca^{2+}; Sigma, St. Louis, MO), supplemented with 5% FCS and 0.1% sodium azide, were stained in a two-step indirect procedure. Cells were first incubated with the monoclonal mouse antibodies BU61 or anti-FLAG followed by incubation with the FITC-conjugated anti-mouse antibody for 20 min at 4 °C. Cytofluorometric analyses were then performed on FACSort (Becton Dickenson, Mansfield, MA). Empty vector transfected cells served as a negative control. The Cell Quest software program was used for collecting and analyzing data. At least 10 000 cells were counted in each experiment, and results were expressed as percent transfection rate (*24*).

Protein Preparation. Cells were washed three times with Tris−saline buffer, pH 8.0 at 4 °C, harvested by scraping in 20 mM Tris, pH 8.0, 50 mM NaCl, and 0.1 mM PMSF, with aprotinin (0.02 KIU/mL), and centrifuged at 300*g* for 5 min at 4 °C. Cells were resuspended in the harvesting buffer. For homogenates and membrane preparations, cells were disrupted in Potter homogenizer and centrifuged at 300*g* for 5 min at 4 °C. Supernatants were used as cell homogenates. Cell membranes were prepared by ultracentrifugation of cell lysates at 150000*g* for 1 h at 4 °C. Pellets were resuspended in 7.5% glycerol and 5 mM Tris-HCl, pH 8.0. Cell lysates were obtained from lysis of COS-7 transfectants induced by incubation with the harvesting buffer containing 1% NP40. Protein was measured according to the Bradford method (*25*).

Affinity Chromatography Purification of FLAG-Tagged Proteins. Cell lysates (500 μL, 15 μg/μL protein) were pooled to equal parts from three different transient transfections of COS-7 cells with either native or one of the N-terminal truncated forms of CD39. All were diluted 1:10 with harvesting buffer containing NP-40, resulting in a final concentration of 0.5%. Tagged CD39 protein was purified on anti-FLAG M2 affinity columns (Kodak Scientific, New Haven, CT) according to the manufacturer's instructions, modified only in that all solutions and buffer were adjusted with NP-40 to a final concentration of 0.5% to keep the membrane protein in soluble form. Concentrated eluates (Centricon 10, Amersham) were used for ATPDase biochemical activity assays and Western analysis. Additional steps with dialysis were required to remove excess detergent, and samples were lyophilized prior to reconstitution for

SDS−PAGE and silver staining. Tagged CD39 mutants were adjusted to the native protein levels by densitometric analysis of Western blots utilizing ImageQuant software (Molecular Dynamics, Sunnyvale, CA). This purification of mutants also provided insights into possible association of proteolytic fragments of CD39 with intact monomeric forms.

ATPDase Assays. Enzyme activity was determined at 37 °C in 1 mL of 5 mM $CaCl_2$, 200 μM substrate (ATP or ADP), and 50 mM Tris, pH 8.0. Reactions were stopped with 0.25 mL of Malachite green reagent and P_i was determined (*26*).

Western Blot Analysis. SDS−polyacrylamide gel electrophoresis (SDS−PAGE) was performed according to Laemmli (*27*). Proteins (5 or 10 μg per lane for cell lysates; equivalent to 1.5 μL of affinity-purified protein) were boiled in sample buffer [2% (w/v) SDS, 10% (v/v) glycerin, 0.001% bromophenol blue in 65 mM Tris, pH 6.8, with or without 1% (v/v) 2-mercaptoethanol as indicated (reducing or nonreducing condition, respectively)] and separated on 10% acrylamide−SDS gel or 4−15% gradient gels and transferred to PVDF membrane (Immobilon P, Millipore, Bedford, MA) by electroblotting (*28*). The latter were then probed with commercial mouse mAb to native CD39 (BU61, AnCell Co., Bayport, MN) or the FLAG epitope (M2, Kodak Scientific) or with polyclonal rabbit antibodies raised against the CD39-derived peptides, aa 102−130 (KY102/130) or aa 202−217 (RO202/217). Bands were visualized using HRP-conjugated goat anti-rabbit IgG or goat anti-mouse IgG (Pierce, Rockford, IL) and the Renaissance Chemiluminesence reagent plus (NEN, Boston, MA) according to the manufacturer's instruction.

Multimeric Analysis after Diamide and Thiol Treatment. Aliquots of homogenates derived from FLAG-tagged CD39 transfected COS-7 cells were incubated in harvesting buffer with varying concentrations of diamide and dithiothreitol for 30 min at room temperature. For the investigation of multimeric patterns, treated homogenates were subjected to Western analysis under nonreducing conditions and patterns compared with standard CD39 preparations.

Tryptic Digestion and Deglycosylation. Aliquots of homogenates derived from FLAG-tagged CD39 transfected COS-7 cells were incubated at 37 °C either in harvesting buffer with 3.3 μg/mL trypsin (Life Technologies, Grand Island, NY) for 5 min or in harvesting buffer supplemented with 0.3% Triton X-100 with 0.25 units of *N*-glycosidase F (Life Technologies, Grand Island, NY) for 12 h (*34*). The reaction for the tryptic digest was stopped with PMSF at a final concentration of 1 mM. Treated and control samples were subjected to Western blot analysis and activity assays as described above.

Statistical Analysis. Data were analyzed by graphical representation and by the Mann Whitney rank sum test where indicated using Sigma Suite Version 2.0 for Windows 95 (Jardel Scientific, San Rafael, CA).

RESULTS

Design of FLAG-Tagged CD39 and Mutant Forms. Hydrophobicity plots (*29*) suggested the presence of two transmembrane regions (TMR) at the N- and C-terminus; an additional hydrophobic region appeared to be localized in the central region of the C-terminal portion in the cysteine-rich area (not shown). The putative TMR were deleted in an individual manner to ascertain the role of the alternative TMR in maintaining membrane association and their effect upon enzymatic activity. Membrane attachment of mutants without both putative TMR was assured by introduction of the GPI-linker signal of DAF at the C-terminus. Native and all CD39 mutants were tagged with the eight amino acid FLAG sequence. Native, ACR deletion mutants, or C-terminal-truncated mutants were tagged at the C-terminus and N-terminal and double-truncated (both N- and C-terminal) mutants at the residual N-terminus. Further truncations at the N-terminal end were designed to remove in a stepwise manner the putative N-terminal TMR (NT Δ-1−37) plus either the ACR-1 (NT Δ-1−61), ACR-1−3 (NT Δ-1−202), or ACR-1−4 (NT Δ-1−220).

The first C-terminal truncation (CT Δ-477−510) removed the TMR, and a subsequent mutant was characterized by the additional loss of ACR-5, plus the C-terminal four cysteine residues (CT Δ-329−510). Further truncations at the C-terminal end sequentially removed four consecutive cysteine residues up to ACR-4 (CT Δ-305−510, CT Δ-286−510, CT Δ-259−510, and CT Δ-221−510). Both putative TMR were removed in two different double-truncated forms of CD39 (DT Δ-1−37/Δ-477−510 and DT Δ-1−37/Δ-221−510). A scheme of generated mutants is presented in Figure 1.

These sequential N-terminal truncations were designed to provide information concerning the role of ACR-1 to -4 in expression and function of CD39. C-Terminal truncations were designed to evaluate the involvement of ACR-5 and the role of disulfide linkages between multiple C-terminal cysteine residues. To determine the effect of isolated effects of ACR-1 or -4, additional deletion mutants lacking ACR-1 (Δ-ACR-1) or ACR-4 (Δ-ACR-4) were designed and then expressed in COS-7 cells.

Biochemical Activity of Native CD39 and Mutants. The ATPase activity of native CD39-transfected COS-7 cell lysates was 337.6 ± 124.9, and the ADPase activity was found to be 242.2 ± 40.3 nmol of P_i min^{-1} mg^{-1}; this normalized ATPase activity was 101 ± 11% and ADPase activity was 94 ± 8% when standardized to values obtained with the tagged CD39 [mean ± standard deviation (SD), three transfections; Figure 2A]. Therefore, the biochemical activity of unmodified CD39 was nearly identical to values obtained with FLAG-tagged protein. These results are derived from assays designed to generate V_{max} with less than 5% of the original substrate (ATP or ADP) hydrolyzed; hence, minimal interference with measurements of ATPase activity will result from the hydrolysis of newly generated ADP.

COS-7 cells following transfection with NT Δ-1−37 and CT Δ-477−510 had slightly lower ADPase activity (77 ± 12% and 68 ± 9%, respectively) and ATPase activity (69 ± 4% and 55 ± 4%, respectively, versus the tagged, intact CD39). The GPI-linked, mutant CD39 with both TMR deleted (termed DT Δ-1−37/Δ-477−510) had marked decreases in nucleotidase activity (ADPase 37 ± 3% and ATPase 34 ± 9% vs tagged CD39; $p < 0.05$. Figure 2A). However, ADPase activity for NT Δ-1−61 (9 ± 6%), NT Δ-1−202 (9 ± 6%), and NT Δ-1−220 (12 ± 9%) together with ATPase activities (22 ± 4%, 20 ± 4%, and 16 ± 6%) were dramatically diminished when compared to tagged native CD39 ($p < 0.001$). COS-7 cell lysates transfected with

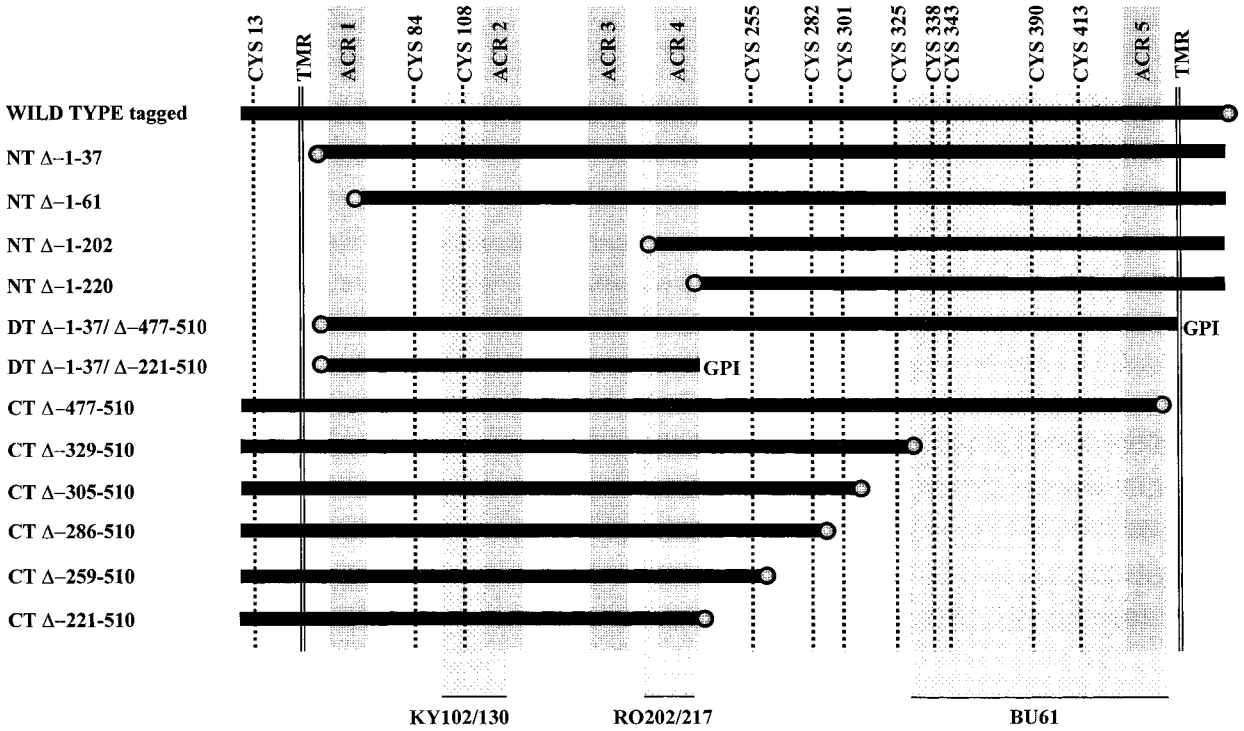

FIGURE 1: Alignment of truncation mutants and FLAG-tagged CD39. Dark gray boxes indicate apyrase conserved regions (ACR) (*2*), and light gray stippled boxes show potential binding epitopes for the specified antibodies. The solid double line indicates the two terminal transmembrane regions (TMR). Dotted lines indicate the cysteine residues. Key: CT, C-terminal truncated; DT, double truncated; NT, N-terminal truncated; circle, FLAG tag; Δ-XX−XXX, the range of residues truncated for the particular mutant; GPI, glycosylphosphatidylinositol anchor.

cDNA encoding mutants with further C-terminal truncations, an extended double-truncated mutant DT Δ-1−37/Δ-221−510, as well as those designed to target Δ-ACR-1 and -4 had no significant ADPase activity (range activity 1−2%). These latter activities were comparable to cells transfected with empty vector.

Immunopurified and reconstituted FLAG-tagged CD39 and the N-terminal truncation mutants were assayed for nucleotidase activity. Normalized NT Δ-1−37 activity was comparable to prior estimates performed on the crude cell lysates (Figure 2B). When compared to purified FLAG-tagged CD39, normalized ADPase activity was markedly diminished for NT Δ-1−61 (6.9 ± 0.2%), NT Δ-1−202 (5.8 ± 0.3%), and NT Δ-1−220 (4.2 ± 0.1%; Figure 2B). ATPase activity was barely detectable for immunoaffinity-purified NT Δ-1−61 (3.0 ± 0.1%), NT Δ-1−202 (3.5 ± 0.1%), and NT Δ-1−220 (2.5 ± 0.1%; Figure 2B). These data, derived from immunopurified mutant forms of CD39, more accurately reflect the loss of ATPDase activity observed with the more substantive truncations at the N-terminus.

Cytofluometric Analysis. COS-7 cells transiently transfected with native and mutant CD39 were analyzed for respective cell surface expression by cytofluometric analysis using BU61 and anti-FLAG mAb. When stained with BU61, tagged native protein, NT Δ-1−37, CT Δ-477−510, and DT Δ-1−37/Δ-477−510 had comparable levels of cell surface expression (52−62%) to the nontagged native CD39 (61 ± 9%; $p > 0.05$; Figure 3).

Other mutant forms of CD39, viz. NT Δ-1−61 (3 ± 1%), NT Δ-1−202 (13 ± 4%), and NT Δ-1−220 (11 ± 3%), were noted to have decreased membrane expression when compared to unmodified protein ($p < 0.001$; Figure 3). Because of anti-CD39 or anti-peptide antibody specificities for regions of the native protein, membrane expression of deletional mutants was determined by using antibodies against the FLAG epitope. When detected with anti-FLAG, expression of C-terminal truncations beyond CT Δ-329−510 was very low, i.e., 2−6%, with the ACR-1 and -4 deletion mutants in the range of 8−14% (data not shown).

Western Blot Analysis. *(A) Characterization of Native CD39*. Lysates of transiently transfected COS-7-cells were analyzed by Western blotting under nonreducing conditions to confirm comparable levels of synthesis of mutant proteins (Figure 4). The 78 kDa full size monomeric form of CD39, a derived 56 kDa fragment (detectable with BU61 and also RO202/217; latter not shown), and the 27 kDa fragment (recognized by KY102/130) were expressed in a comparable manner for both unmodified and FLAG-tagged proteins (Figure 4). Small amounts of a 42 kDa fragment were also visualized with BU61 with longer exposure times (data not shown). None of these derived forms of the monomeric form of CD39 were recognized by the anti-FLAG antibodies, suggesting removal of this epitope in a posttranslational manner.

The predominant monomeric form was observed to undergo multimerization to form dimers, trimers, tetramers, and higher oligomers observed with anti-FLAG and KY102/130 (Figure 4) as well as with RO202/217 (not shown). Oligomer formation was observed for both tagged and nontagged native CD39 (Figure 4) and occurred only under nonreducing conditions as detected with anti-FLAG (not shown). Greater cross-linking by disulfide bridging between cysteine residues following exposure to diamide resulted in a shift of the pattern toward the higher multimers. In contrast,

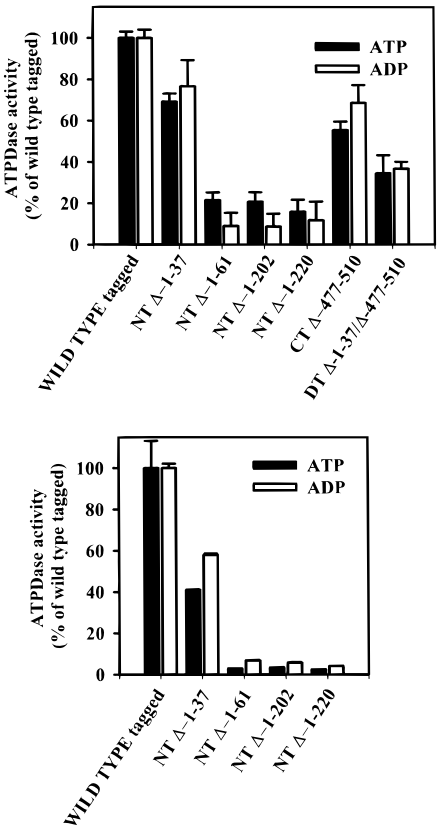

FIGURE 2: Biochemical activity of FLAG-tagged CD39 or truncation mutants as defined in Figure 1. Hydrolysis of ADP and ATP was determined by measuring phosphate release using the Malachite green technique. (A, top) Lysates of transfected COS-7 cells. The vertical axis shows normalized activity as a percentage value of ATPase (325.0 ± 102.3 nmol of P_i mg^{-1} min^{-1}) and ADPase (263.3 ± 61.2 nmol of P_i mg^{-1} min^{-1}) results obtained with the FLAG-tagged intact CD39. (B, bottom) CD39 FLAG-tagged and mutants, affinity purified from transfected COS-7 cells with normalized activity again expressed on the vertical axis.

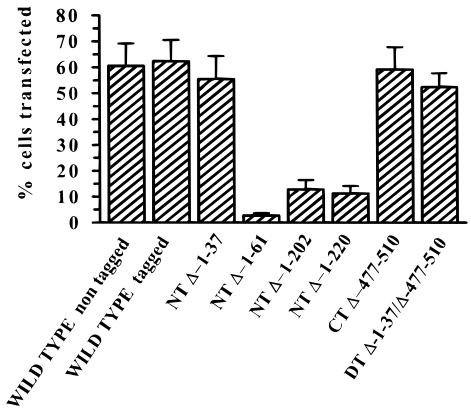

FIGURE 3: Cytofluorometric analysis of COS-7 cells transiently transfected with native CD39 and a selection of mutants. The percentage of viable cells expressing CD39 epitopes recognized by BU61 is shown on the vertical axis.

treatment of CD39 preparations with dithiotreitol (DTT) or β-mercaptoethanol (ME) resulted in a loss of the multimeric pattern. The reduced monomeric CD39 comprised a doublet with a thin lower band immediately below the major 78 kDa isoform, which was not detected in samples showing multimerization (not shown).

Western blot patterns for affinity-purified CD39 were comparable to nonpurified native CD39 including a 27 kDa band detectable with KY102/130 in the presence or absence of β-ME, with the 56 kDa form recognized by BU61 under nonreducing conditions (Figure 5) and RO202/217 (data not shown). Both of these lower M_r isoforms were not detectable with anti-FLAG antibody. The double band observed under nonreducing conditions, at approximately 150 kDa, was due to affinity gel derived mouse IgG. Silver staining of purified native CD39 after lyophilization revealed one strong band migrating on the level of the full size monomeric CD39 (Figure 5).

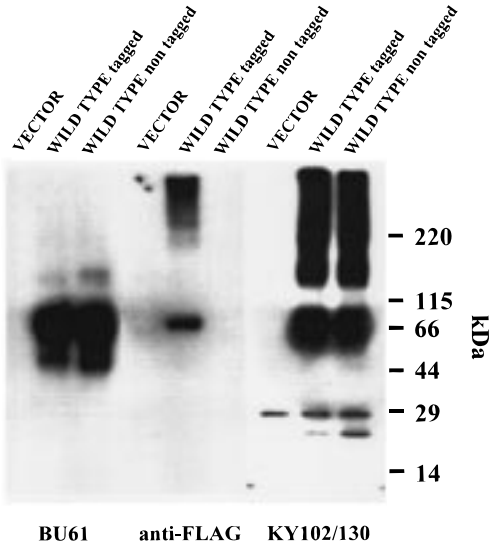

FIGURE 4: Western blotting of lysates of transiently transfected COS-7 cells for FLAG-tagged and native (nontagged) CD39. Blots were developed with monoclonal (BU61) and polyclonal (KY102/130) antibodies to human CD39 and monoclonal antibody M2 detecting the FLAG epitope (anti-FLAG). A total of 8 μg of protein was loaded on each lane. The nonspecific band at 29 kDa recognized by KY102/130 was also observed with empty vector transfected cells (VECTOR).

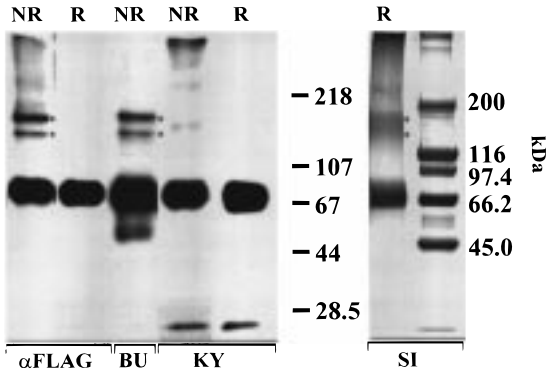

FIGURE 5: Western blot analysis of affinity-purified FLAG-tagged CD39 preparations. Samples were subjected to SDS−PAGE under nonreducing (NR) and reducing (R) conditions. CD39 was detected with anti-FLAG M2 (αFLAG), monoclonal anti-CD39 BU61 (BU), and KY102/130 (KY); samples were also subjected to silver staining (SI). Molecular standards are shown adjacent to the SI purified proteins. An asterisk designates coeluted murine Ig.

(B) Characterization of Deletional Mutants. Isolated deletions at either ACR-1 or -4 resulted in generally diminished levels of protein expression that required longer development times for visualization (Figure 6). However, the monomeric forms of native CD39 and the ACR deletion mutants were recognized by BU61 and KY102/130. The CD39 Δ-ACR-4 mutant was not detectable with RO202/217,

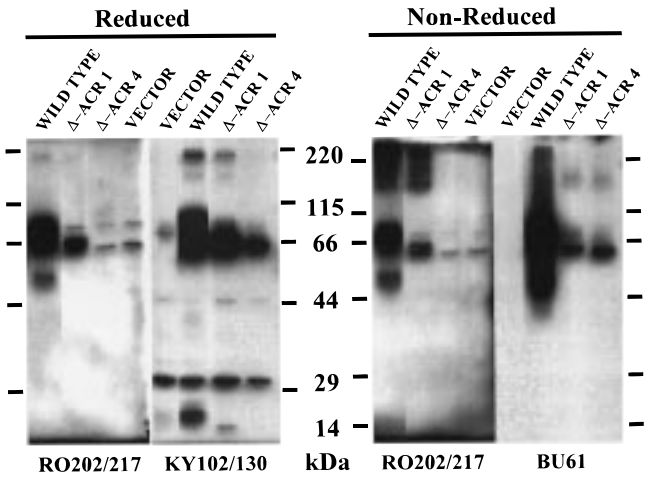

FIGURE 6: Western blotting of COS-7 cells transfected with FLAG-tagged native CD39, deletion mutants ACR-1 (Δ-ACR 1) and ACR-4 (Δ-ACR 4), or empty vector. Deletional mutants of CD39 targeting ACR-1 and -4 were subjected to SDS−PAGE under nonreducing and reducing conditions. Blots were developed with polyclonal anti-CD39 RO202/217, KY102/130, or monoclonal BU61.

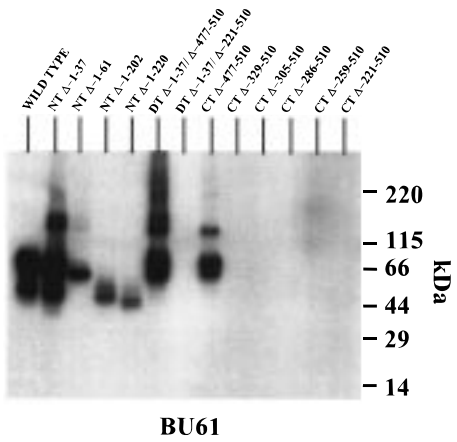

FIGURE 7: Native CD39 N- and C-terminal truncation mutants were subjected to SDS−PAGE under nonreducing conditions. Western blots were developed with anti-human CD39 monoclonal antibody (BU61). The C-terminal truncations beyond the TMR removed the epitopes recognized by this monoclonal antibody.

in keeping with the deletion of the predicted major part of the epitope. Two faint bands at 66 and 80 kDa detected by RO202/217 were also detectable in empty vector transfected COS-7 cells and thus considered nonspecific. The 56 kDa fragment (recognized by BU61 or RO202/217) was not observed in ACR-1 or -4 deleted forms of CD39. The 27 kDa fragment (recognized by KY102/130) was observed in native CD39 and not in ACR-4 deleted forms; a relatively smaller Δ-ACR-1 isoform (25 kDa) was observed in keeping with the deletion within ACR-1. Multimeric patterns for native CD39 and Δ-ACR-1 were visualized by RO202/217 and also for Δ-ACR-4 by BU61 under nonreducing conditions; multimers were also observed for ACR deleted forms of CD39 by anti-FLAG and were comparable to native protein (data not shown).

(C) Characterization of Truncation Mutants. Native CD39 with and without the FLAG, all N-terminal truncated mutants, CT Δ-477−510, and DT Δ-1−37/Δ-477−510 were visualized under nonreducing conditions with BU61 (Figure 7). The expression of NT Δ-1−37, DT Δ-1−37/Δ-477−510, and CT Δ-477−510 as detected with BU61 was comparable to unmodified enzyme; NT Δ-1−61 had lower expression that further diminished with greater N-terminal truncations. CD39 mutants with the C-terminal truncation Δ-329−510 and beyond were not detected in these Western blots, suggesting that BU61 recognized an epitope between amino acids 329 and 477. No detection of CD39 or mutants occurred with BU61 under reduced conditions, suggesting that disulfide linkages and their role in generating the tertiary structure were important for the epitope (data not shown). Anti-FLAG antibody did not react with the 56 kDa isoforms observed with BU61 and RO202/217 (Figures 6 and 7) or any other degradation product in the mutant and native CD39 (Figure 8).

In addition to the full-sized monomer, a 56 kDa isoform was observed in native and NT Δ-1−37 (Figure 7). BU61 detected CT Δ-477−510 and DT Δ-1−37/Δ-477−510 truncated mutants as double bands. This size heterogeneity was due to glycosylation variation (see below). KY102/130 detected a 27 kDa form only in native enzyme and CT Δ-477−510. The latter antibody detected a full size monomer in all truncational mutants except NT Δ-1−202 and NT Δ-1−220 (that lack the epitope for KY102/130; data not shown).

Features of Multimeric Forms of Native and Mutant CD39. BU61 detected multimerization in predominantly truncation mutants lacking one or both TMR (Figure 7). Oligomers of unmodified CD39 or further N-terminal truncations reacted only minimally with BU61 in contrast to anti-FLAG (Figure 8), KY102/130 (Figure 4), and RO202/217 (Figure 6). Under reducing conditions, anti-FLAG detected CD39 as a monomer (Figure 8). The patterns for the full size monomer under reducing conditions were comparable for all truncated CD39 variations with detection by either KY102/130, anti-FLAG, or RO202/217 (data for the latter not shown). Under nonreducing conditions, most forms of CD39 were detected predominantly as oligomers. All truncated forms of CD39 underwent multimerization although to a reduced extent for NT Δ-1−202, NT Δ-1−220, and DT Δ-1−37/Δ-221−510 (Figure 8). Mutants that did not form these very high multimers shared several characteristics. These included absence of either three N-terminally located cysteine residues or all of the C-terminal cysteine residues plus the intracytoplasmic N-terminal cysteine (Figure 1).

Increases in the 56 kDa Isoform Are Associated with Augmentation of Enzymatic Activity. Following limited proteolysis of native CD39 with trypsin, Western blot analysis was performed with BU61 (nonreducing conditions) and with KY102/130 (reducing conditions) as depicted in Figure 9. Limited proteolysis of native CD39 resulted in conversion of the 78 kDa form to the 56 kDa band (recognized by BU61) and the 27 kDa band (recognized by KY102/130), respectively. Normalized ATPDase activity was substantively boosted (by 190.1 ± 2%) following limited proteolysis with trypsin and the associated degradation to the lower M_r derivatives (Figure 9). Similar changes in activity and conversion to the M_r 56 000 isoform were noted with partially purified human umbilical vessel ATPDase preparations undergoing tryptic digestion (data not shown).

Deglycosylation of Native and Selected Mutants of CD39. Native CD39 and selected truncated mutants were treated

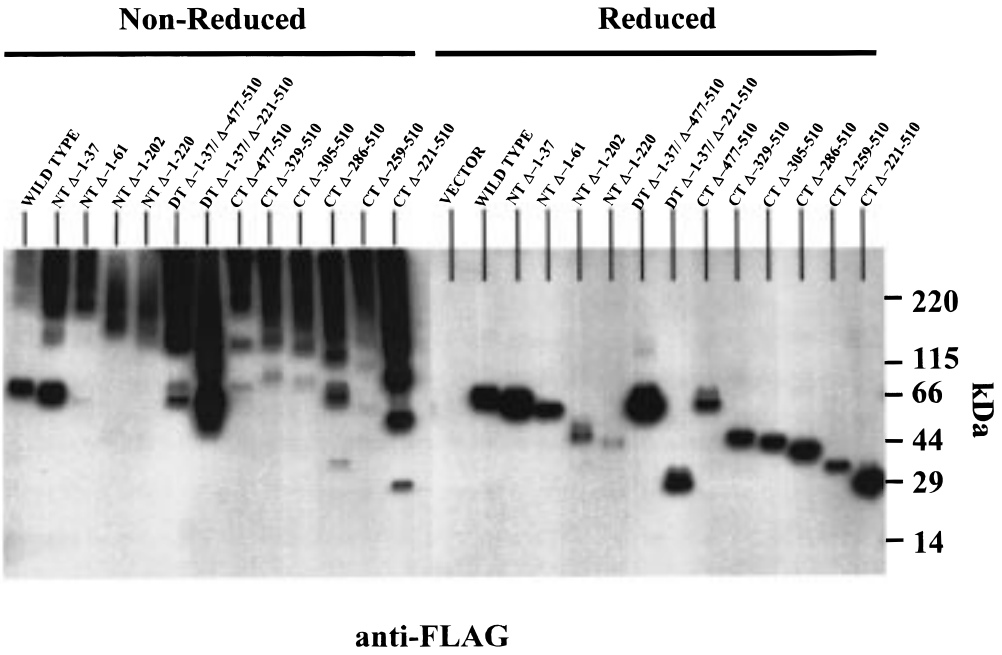

FIGURE 8: Native and mutant forms of CD39 were subjected to SDS−PAGE under both reducing and nonreducing conditions. Western blots were developed with anti-FLAG Ab M2 to confirm the presence of C-terminal truncation mutants and evaluate multimeric patterns.

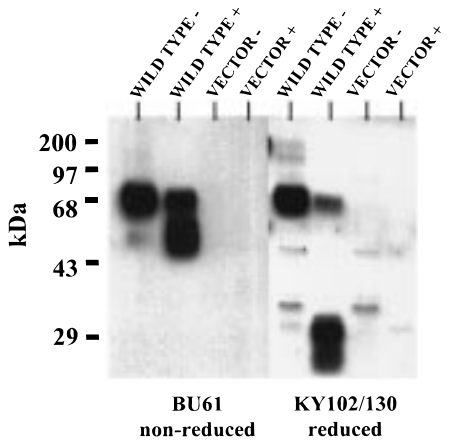

FIGURE 9: Trypsin-treated (+) and nontreated (−) cell lysates from transfected COS-7 cells were subjected to SDS−PAGE under both reducing and nonreducing conditions, and Western blots were developed by BU61 or KY102/130 to show conversion of intact monomeric CD39 to the major derivatives. COS-7 cells were transfected with FLAG-tagged CD39 or empty vector (VECTOR). Cell lysates were performed as described in Experimental Procedures.

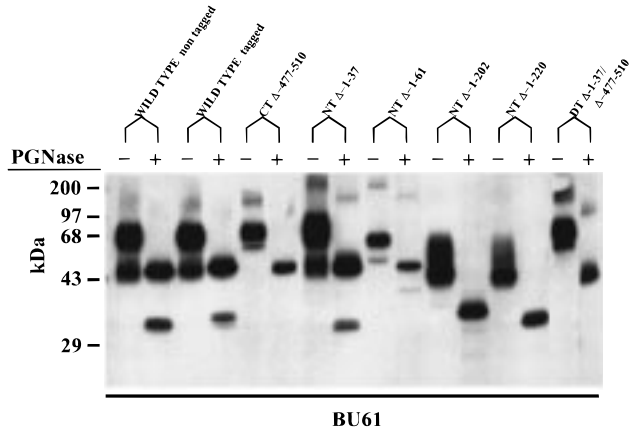

FIGURE 10: CD39 and mutants designated as in Figure 1 underwent enzymatic deglycosylation with PNGase. Proteins were then submitted to SDS−PAGE under nonreducing conditions and Western blotted using BU61. Blots clearly show the presence of the intact monomeric protein and the major degradation fragment of CD39 in native and NT Δ-1−37 (weak reaction for NT Δ-1−61). Following deglycosylation, only one protein isoform can be recognized for both CT Δ-477−510 and DT Δ-1−37/Δ-477−510.

with *N*-glycosidase F (PGNase) to remove GlycNAcβ_1−GlycNAc attachments at N-linked glycosylation sites. Deglycosylated proteins migrated proportionally with appropriate decreases in relative molecular mass (Figure 10). The double band seen for CT Δ-477−510 and DT Δ-1−37/Δ-477−510 became one single band following PGNase treatment (Figure 10). These data confirm that doublets of CT Δ-477−510 and DT Δ-1−37/Δ-477−510 are glycosylation variations. Similar patterns were observed with a metabolic inhibitor of protein glycosylation (swainsonine; data not shown). Biochemical activity was essentially unaltered by glycosylation status (not shown).

DISCUSSION

We have previously shown that vascular EC rapidly lose ATPDase activity following reperfusion injury (*30*) or other inflammatory reactions (*22*). As the local administration of soluble apyrase has beneficial effects abrogating platelet sequestration within the graft vasculature of transplanted organs (*31*), we have considered that targeted expression of high levels of stable and active ATPDase might be an effective therapeutic intervention for vascular inflammation. To this end, we have generated a series of truncated and deletional mutants of CD39 (Figure 1) to determine the possible designs of substantially smaller derivatives of CD39 that could be then further modified to heighten enzymatic (preferentially ecto-ADPase) activity and also increase resistance to oxidant stress.

We found that insertion of FLAG tag did not substantively change ADPase or ATPase activity of the native CD39/ATPDase and did not substantially influence protein antigenic structure; the patterns for the full size monomer (78

Table 2: Deduced Sequence Alignment of the C-Termini of CD39 and Apyrase-like Proteins from Different Organisms and Species[a]

		ACR 5
human	CD39	WEHIHFIGKIQGSDAGWTLGYMLNLTNMIPAEQPLSTPL
human-brain	ecto-apyrase	WPQIHFEKEVGNSSIAWSLGYMLSLTNQIPAESPLIRLP
bovine	CD39	WKNIHFMNKVRSTDVGWTLGYMLNLTNKIPAEEPMSPPL
murine	CD39	WEQIHFMGKIKDSNAGWTLGYMLNLTNMIPAEQPLSPPL
rat	CD39	WDQIHFMGKIKDSNAGWTLGYMLNLTNMIPAEQPLSPPL
chicken	ATPDase	WSNIHFSQKAGNADIGWTLGFMLNLTNMIPTEALEHVKG
potato	apyrase	TVIHDVQYKNYLVGAAWPLGCAIDLVSSTTNKIRVASS*
human	UDPase	YKSLKTALQVYDKEVQWTLGAILYRTRFLPLRDIQQEAF
yeast	GDPase	QRELRTGKKIANKEIGWCLGASLPLLKADNWKCKIQSA*

[a] GenBank Accession Numbers: Human CD39, S73813; human brain ectoapyrase, AF034840; bovine CD39, AF005940; chicken ATPDase, AF041355; rat CD39, U81295; murine CD39, AF037366; potato apyrase, P80595; human UDPase, AB002390; yeast GDPase, P32621. The dark shaded areas indicate exact matches, the light shaded areas mark highly conserved residues of ACR-5, and asterisks indicate the N-terminal end of the sequence.

kDa) and the 56 and 27 kDa forms as well as the pattern of multimerization were comparable for both native and FLAG-tagged proteins on Western blotting. Purification of selected mutants by FLAG-epitope affinity chromatography was undertaken for normalization of antigen levels. These purified mutants permitted the determination of relative ATPDase enzymatic activities given potential changes in immunogenic epitopes as determined by antibodies to CD39 with varying degrees of protein synthesis and expression of the various mutants observed (Figures 2B and 5).

Our data demonstrated that either the N- or C-terminus alone was able to localize CD39 in the cell membrane with the appropriate extracellular domains accessible to antibodies and cytofluorometric analysis as predicted by hydrophobicity plots (*5*). Anchoring mediated by the N-terminal TMR seemed to be more robust than by the C-terminal counterpart; specifically, only N-terminal truncated forms were found as solubilized monomeric and dimeric forms in conditioned media of transfected COS-7 cell cultures (data not shown). The independent development of a double-truncated CD39 mutant without a GPI linker and the recent demonstration of solubility have also confirmed that the central hydrophobic area alone is insufficient for membrane association (*32*). This observation has been recently confirmed by another group for the rat ectoapyrase (*33*).

Native CD39 and the mutants with truncation of either the N- or C-terminal TMR, adjacent to ACR-1 or ACR-5, respectively, were well expressed on the cell membranes. Further truncation or deletional mutations involving only one individual or several ACR-1 to -5 led to substantially diminished surface expression, possibly relating to impaired protein folding and failure of transport. Truncation of the N-terminus involving the TMR and at least ACR-1 resulted in intracellular localization of these mutants. Electron microscopy studies confirmed failure of plasma membrane translocation of CD39 truncational mutants lacking ACR-1 (Agnes Kittel, Budapest, Hungary personal communication). Deletion of ACR-1 or -4 was also accompanied by somewhat decreased expression, indicating a potential requirement of these regions for appropriate protein folding and full expression of CD39 (Figure 6).

The only mutants to exert ATPDase activity comparable to that of the native enzyme were those with either one or the other terminal TMR absent (Figure 2). Dissociation of high levels of ATPase from ADPase activity or vice versa was not observed in any of the mutants tested. Deletion of both TMR and linkage of DT Δ-1−37/Δ-477−510 to the membrane did decrease ATPDase activity relative to native CD39 but not to the extent observed with removal of the ACR (Figure 2A). During the final preparation of this paper, Wang and colleagues also reported that rat ectoapyrase mutants lacking both TMR had some decreases in ATPDase activity (*33*), in keeping with our functional observations with similar mutations of human CD39.

The determination that the N-terminal ACR (specifically ACR-1) was necessary for ATPDase enzymatic activity was initially surprising. We had previously proposed that ACR-4 was the most important candidate location for the formation of the active site in the light of sequence data from the pig pancreatic ATPDase that seemed not to have ACR-1 to -3 (*1, 9*); additionally, initial targeting within ACR-4 had substantially abolished enzyme activity. However, mutations specifically targeting ACR-1 had inhibitory effects similar to those disrupting ACR-4, and it is possible that such mutations could provoke structural rearrangements that could mask the true catalytic site; comparable alterations could arise following removal of the ACR-2 and -3. The separate truncations of the C-terminal regions removing the putative ACR-5 (*14*) also markedly inhibited both ATPase and ADPase activity. Upon examination of this region in more detail, it became clear that ACR-5 was highly conserved among CD39 proteins (*6, 34*) and is also seen in human UDPase (*35*), yeast GDPase, and potato apyrase (*2*) (Table 2).

Analysis of labeled and truncated mutants by Western blotting provided valuable information on protein structure, posttranslational modifications, and their potential influence on enzyme activity. Importantly, truncation mutants of CD39 lacking amino acids 329−477 were not recognized by BU61 (Figure 7), indicating that this monoclonal antibody recognized an epitope in the C-terminal region. We were also able to confirm the expected specificities of the polyclonal antibodies used to identify CD39 fragments (Figures 4 and 6). The generation of a 56 kDa fragment, recognized by polyclonal antibody, RO202/217 raised to a peptide sequence within ACR-4 (not shown) and BU61, was observed in mutants with deletions of the N-terminus to amino acid 61

(Figure 7). N-Terminal truncations of CD39 beyond ACR-1 did not demonstrate this additional band. The 27 kDa fragment recognized by KY102/130 (Figure 4) was detected to a minor degree in the C-terminal truncated forms of CD39 that preserved the ACR-5 (not shown).

This detection of the 56 kDa fragment by RO202/217 suggested posttranslational modifications involving limited proteolysis of the native protein with specific cleavages approximate to ACR-4, as previously suggested for the pancreas ATPDase isoform (*9*). The 27 kDa proteolytic fragment recognized by KY102/130 has been also noted in preparations of human umbilical cord vessels and porcine pancreatic ATPDase (Jean Sévigny, unpublished observations), in keeping with an association with the 56 kDa membrane-bound remaining fraction (Figure 5). The summed molecular weights of approximately 83 000 (viz. 56 000 + 27 000) further support the contention that these isoforms are generated by limited proteolysis. Conclusively, these modifications could also be reproduced by limited proteolysis with trypsin, suggesting a cleavage site at Lys-188 or -192 just proximal to the N-terminal area of ACR-4 (Figures 1 and 9). M2 anti-FLAG did not detect the 56 kDa C-terminal fragment of the native CD39 that was FLAG tagged, suggesting the existence of another C-terminal (co)cleavage site.

Importantly, such limited tryptic digestion of CD39 boosted basal ATPDase levels. The expression of trypsin-related serine proteases by vascular EC (*36*) suggests that modification of CD39 could be related to local activation responses that could be relevant to inflammatory processes within vasculature (*37*, *38*). In addition, multimer formation was dramatically decreased in preparations of CD39 that had undergone tryptic digestion (data not shown). This described proteolytic modification of CD39 appeared dependent on the integrity of ACR-4 and -5 and was largely independent of both terminal TMR and ACR-1. In the latter case of Δ-ACR-1, a 25 kDa form of CD39 specifically detected with KY102/130 indicated a faster migrating analogue of the 27 kDa fragment (Figure 6; not shown). However, the 56 kDa fragment of the cleaved protein was not detectable within the mutant Δ-ACR-1 by either RO202/217 or BU61 (Figure 6). The failure to detect this fragment in Δ-ACR-1 could be due to impaired association to the intact native isoform, leading to increased solubility and/or more susceptibility to further proteolytic degradation. The same mechanism was likely responsible for the missing 56 kDa analogue in the C-terminal TMR truncation mutant (CT Δ-477−510) (Figure 7).

Purification of the native intact protein by affinity chromatography resulted in copurification of the 56 and 27 kDa forms (Figure 5) that were demonstrated not to be FLAG tagged (Figures 4 and 8). Proteolytic cleavage of native protein on the affinity column despite the presence of protease inhibitors was considered unlikely, as in this instance the proteolytic fragments should not have been held on the affinity gel because of the absence of the FLAG tag. Since the purity of the preparation was confirmed by silver staining (Figure 5), our observations are most likely explained by the prior association of fragments to other full-sized CD39 monomers and potentially their oligomeric forms.

BU61 although recognizing monomeric and 56 kDa forms did not readily interact with the CD39 multimers despite their clear demonstration by antibodies to the FLAG epitope and regions within the N-terminal zones (Figures 4, 7, and 8). For the N-terminal truncation mutants, differences in detection of multimeric patterns between BU61 and anti-FLAG were also observed (Figures 7 and 8). These patterns suggested that high M_r oligomer formation of CD39 may be dependent upon disulfide linkages between cysteines 338 and 413 contained within the native C-terminus. As determined with the generation of truncation mutants, the formation of the highest molecular weight oligomers with CD39 (tetramers and higher) was shown to be dependent upon at least two of the following cysteine groups: first, cysteines beyond position 255 in the C-terminal region with Cys-13, and second, cysteines within the N-terminus (residues 84 and 104). The intracytoplasmic cysteine within the N-terminus also seemed to promote intermolecular linkages in the mutant CT Δ-221−510 (lacking the region to the C-terminus of ACR-4) when contrasted to DT Δ-1−37/Δ-221−510 (Figure 8).

A lower monomeric form of CD39 appeared to be predominantly utilized in the process of oligomerization (not shown) and may be analogous to the glycosylation variant of the CT Δ- 477−510 mutant truncated at the C-terminus as well as in DT Δ-1−37/Δ-477−510 truncated at both TMRs (Figures 7 and 10). Although ATPDase is known to be substantively glycosylated, the extent of this did not appear to influence enzymatic activity (not shown and ref *39*). Oligomer formation was also not influenced by deletional modifications within ACR-1 or -4 (Figure 6), but intermolecular links were generally boosted by deletions of TMR. The formation of oligomers was promoted by cysteine cross-linking by the specific action of diamide and abolished by dithiols and mercaptoethanol (*13*). These data suggest that the multimerization process that we observed was dependent upon the formation of disulfide bridges and was considered in keeping with prior observations with other ecto-ATPases and ATPDases (*19*, *40*). Initial observations with chicken gizzard ecto-ATPase suggested that agents and conditions stabilizing ecto-ATPase oligomers would stimulate enzymatic activity (*40*). More recent reports have shown that although cross-linking by intermolecular disulfide bonds of chicken stomach ectoapyrase appears to induce homodimer formation, the functional result was inhibition of enzymatic activity (*19*). These differences were ascribed to different quaternary structural stability of the two enzymes that require further evaluation (*19*). Certainly, these results also do not exclude a direct effect of reducing agents upon intramolecular CD39 disulfide bonds with perturbation of the active site. Wang et al. have noted that recombinant rat ectoapyrase could form a tetramer that did not appear to require intermolecular disulfide bonds (*33*). These and other observations examining CD39 multimer formation dependent upon disulfide bonds (*19*, *40*) should be considered in the light of prior data derived from gel filtration and ^{60}Co irradiation inactivation techniques which suggest that mammalian ATPDases, including those of the rat placenta and kidney, exist as active monomeric forms under nondenaturing conditions (*41*−*43*). Thus, multiple factors may influence enzymatic activity associated with the formation of multimers including the effects of limited proteolysis, as alluded to above.

In conclusion, we have demonstrated that major portions of CD39 with the preservation of ACR-1, ACR-4, and the C-terminus including ACR-5 are necessary for maintenance of substantial enzymatic activity, structural integrity, and

protein expression on cell membranes. Proteolytic degradation of native protein has been modeled by limited tryptic digestion of both recombinant and purified forms of human CD39. ATPDase enzymatic activity was boosted by limited proteolysis but was not affected by deglycosylation. The derivatives resulting from proteolytic cleavage appear to be associated with the native CD39 isoform and indicate a requirement for at least the major ACRs denoted above. Our demonstration that at least three ACRs are important for enzymatic structure and function provides further insights that may facilitate the design of stable soluble forms of CD39 with high levels of ATPDase activity.

ACKNOWLEDGMENT

We are grateful to Dr. Fritz H. Bach for his many contributions to our research efforts.

REFERENCES

1. Kaczmarek, E., Koziak, K., Sevigny, J., Siegel, J. B., Anrather, J., Beaudoin, A. R., Bach, F. H., and Robson, S. C. (1996) *J. Biol. Chem. 271*, 33116−33122.
2. Handa, M., and Guidotti, G. (1996) *Biochem. Biophys. Res. Commun. 218*, 916−923.
3. Wang, T.-F., and Guidotti, G. (1996) *J. Biol. Chem. 271*, 9898−9901.
4. Marcus, A. J., Broekman, M. J., Drosopoulos, J. H. F., Islam, N., Alyonycheva, T. N., Safier, L. B., Hajjar, K. A., Posnett, D. N., Schoenborn, M. A., Schooley, K. A., Gayle, R. B., and Maliszewski, C. R. (1997) *J. Clin. Invest. 99*, 1351−1360.
5. Maliszewski, C. R., Delespesse, G. J., Schoenborn, M. A., Armitage, R. J., Fanslow, W. C., Nakajima, T., Baker, E., Sutherland, G. R., Poindexter, K., Birks, C., et al. (1994) *J. Immunol. 153*, 3574−3583.
6. Zimmermann, H., Braun, N., Kegel, B., and Heine, P. (1998) *Neurochem. Int. 32*, 421−425.
7. Plesner, L. (1995) *Int. Rev. Cytol. 158*, 141−214.
8. Knowles, A. F., Isler, R. E., and Reece, J. F. (1983) *Biochim. Biophys. Acta 731*, 88−96.
9. Sevigny, J., Cote, Y. P., and Beaudoin, A. R. (1995) *Biochem. J. 312*, 351−356.
10. Sevigny, J., Levesque, F. P., Grondin, G., and Beaudoin, A. R. (1997) *Biochim. Biophys. Acta 1334*, 73−88.
11. Sevigny, J., Picher, M., Grondin, G., and Beaudoin, A. R. (1997) *Am. J. Physiol.—Lung Cell. Mol. Physiol. 16*, L939−L950.
12. Vasconcelos, E. G., Nascimento, P. S., Meirelles, M. N., Verjovski, A. S., and Ferreira, S. T. (1993) *Mol. Biochem. Parasitol. 58*, 205−214.
13. Asai, T., Miura, S., Sibley, L. D., Okabayashi, H., and Takeuchi, T. (1995) *J. Biol. Chem. 270*, 11391−11397.
14. Vasconcelos, E. G., Ferreira, S. T., de Carvalho, T. M. U., de Souza, W., Kettlun, A. M., Mancilla, M., Valenzuela, M. A., and Verjovski-Almeida, S. (1996) *J. Biol. Chem. 271*, 22139−22145.
15. Komoszynski, M. A. (1996) *Comp. Biochem. Physiol. B: Biochem. Mol. Biol. 113*, 581−591.
16. Marcus, A. J., Safier, L. B., Hajjar, K. A., Ullman, H. L., Islam, N., Broekman, M. J., and Eiroa, A. M. (1991) *J. Clin. Invest. 88*, 1690−1696.
17. Marcus, A. J., and Safier, L. B. (1993) *FASEB J. 7*, 516−522.
18. Zimmermann, H. (1992) *Biochem. J. 285*, 345−365.
19. Carl, S. A. L., Smith, T. M., and Kirley, T. L. (1998) *Biochem. Mol. Biol. Int. 44*, 463−470.
20. Kegel, B., Braun, N., Heine, P., Maliszewski, C. R., Zimmermann, H. (1997) *Neuropharmacology 36*, 1189−1200.
21. Robson, S. C., Daoud, S., Begin, M., Cote, Y. P., Siegel, J. B., Bach, F. H., and Beaudoin, A. R. (1997) *Blood Coagulation Fibrinolysis 8*, 21−27.
22. Robson, S. C., Kaczmarek, E., Siegel, J. B., Candinas, D., Koziak, K., Millan, M., Hancock, W. W., and Bach, F. H. (1997) *J. Exp. Med. 185*, 153−163.
23. Ho, S. N., Hunt, H. D., Horton, R. M., Pullen, J. K., and Pease, L. R. (1989) *Gene 77*, 51−59.
24. Schulte am Esch, J., Siegel, J. B., Cruz, M., Anrather, J., and Robson, S. C. (1997) *Blood 90*, 4425−4437.
25. Bradford, M. M. (1976) *Anal. Biochem. 72*, 248−254.
26. Baykov, A. A., Evtushenko, O. A., and Avaeva, S. M. (1988) *Anal. Biochem. 171*, 266−270.
27. Laemmli, U. K. (1970) *Nature 227*, 680−685.
28. Towbin, H., Staehelin, T., and Gordon, J. (1979) *Proc. Natl. Acad. Sci. U.S.A. 76*, 4350−4354.
29. Kyte, J., and Doolittle, R. F. (1982) *J. Mol. Biol. 157*, 105−132.
30. Candinas, D., Koyamada, N., Miyatake, T., Siegel, J., Hancock, W. W., Bach, F. H., and Robson, S. C. (1996) *Thromb. Haemostasis 76*, 807−812.
31. Koyamada, N., Miyatake, T., Candinas, D., Hechenleitner, P., Siegel, J., Hancock, W. W., Bach, F. H., and Robson, S. C. (1996) *Transplantation 62*, 1739−1743.
32. Gayle, R. B., Maliszewski, C. R., Gimpel, S. D., Schoenborn, M. A., Caspary, R. G., Richards, C., Brasel, K., Price, V., Drosopoulos, J. H. F., Islam, N., Alyonycheva, T. N., Broekman, M. J., and Marcus, A. J. (1998) *J. Clin. Invest. 101*, 1851−1859.
33. Wang, T. F., Ou, Y., and Guidotti, G. (1998) *J. Biol. Chem. 273*, 24814−24821.
34. Chadwick, B. P., and Frischauf, A. M. (1997) *Mamm. Genome 8*, 668−672.
35. Wang, T. F., and Guidotti, G. (1998) *J. Biol. Chem. 273*, 11392−11399.
36. Koshikawa, N., Nagashima, Y., Miyagi, Y., Mizushima, H., Yanoma, S., Yasumitsu, H., and Miyazaki, K. (1997) *FEBS Lett. 409*, 442−448.
37. Bach, F. H., Ferran, C., Soares, M., Wrighton, C. J., Anrather, J., Winkler, H., Robson, S. C., and Hancock, W. W. (1997) *Nat. Med. 3*, 944−948.
38. Hwa, J. J., Ghibaudi, L., Williams, P., Chintala, M., Zhang, R., Chatterjee, M., and Sybertz, E. (1996) *Circ. Res. 78*, 581−588.
39. Christoforidis, S., Papamarcaki, T., and Tsolas, O. (1996) *Biochim. Biophys. Acta 1282*, 257−262.
40. Stout, J. G., and Kirley, T. L. (1996) *Biochemistry 35*, 8289−8298.
41. Picher, M., Cote, Y. P., Beliveau, R., Potier, M., and Beaudoin, A. R. (1993) *J. Biol. Chem. 268*, 4699−4703.
42. Pieber, M., Valenzuela, M. A., Kettlun, A. M., Mancilla, M., Aranda, E., Collados, L., and Traverso, C. A. (1991) *Comp. Biochem. Physiol. B: Comp. Biochem. 100*, 281−285.
43. Valenzuela, M. A., Kettlun, A. M., Sandoval, S., Garcia, L., Mancilla, M., Neckelmann, G., Chayet, L., Alvarez, A., Cuevas, F., Collados, L., Espinosa, V., Traversocori, A., Bravo, I., Acevedo, C. G., and Aranda, E. (1996) *Braz. J. Med. Biol. Res. 29*, 589−597.

BI982426K